CrossMark

RETINAL DISORDERS

Functional changes at the preferred retinal locus in subjects with bilateral central vision loss

Arun Kumar Krishnan[1,2] ⬤ · Harold E. Bedell[2]

Abstract

Purpose Subjects with bilateral central vision loss (CVL) use a retinal region called the preferred retinal locus (PRL) for performing various visual tasks. We probed the fixation PRL in individuals with bilateral macular disease, including age-related macular degeneration (AMD) and Stargardt disease (STGD), for localized sensitivity deficits.

Methods Three letter words at the critical print size were presented in the NIDEK MP-1 microperimeter to determine the fixation PRL and its radial retinal eccentricity from the residual fovea in 29 subjects with bilateral CVL. Fixation stability was defined as the median bivariate contour ellipse area (BCEA) from 3 fixation assessments. A standard 10–2 grid (68 locations, 2° apart) was used to determine central retinal sensitivity for Goldmann size II test spots. Baseline and follow-up supra-threshold screening of the fixation PRL for localized sensitivity deficits was performed using high density (0.2° or 0.3° apart) 0 dB Goldmann size II test spots. Custom MATLAB code and a dual bootstrapping algorithm were used to register test-spot locations from the baseline and follow-up tests. Locations where the 0 dB test spots were not seen on either test were labeled as micro-scotomas (MSs).

Results Median BCEA correlated poorly with the radial eccentricity of the fixation PRL. Mean (±SD) sensitivity around the PRL from 10–2 testing was 4.93 ± 4.73 dB. The average percentage of MSs was similar for patients with AMD (25.4%), STGD (20.3%), and other etiologies of CVL (27.1%).

Conclusions The fixation PRL in subjects with bilateral CVL frequently includes local regions of sensitivity loss.

Keywords Micro-perimetry · Central vision loss · Macular degeneration · Preferred retinal locus (PRL) · Micro-scotomas

✉ Arun Kumar Krishnan
arunopto@gmail.com

1   Envision Research Institute, Envision Inc., 610 N Main Street, Wichita, KS 67203, USA

2   University of Houston, College of Optometry, Houston, Texas, USA

Introduction

Age-related macular degeneration (AMD) is among the most common cause of permanent visual impairment in developed countries such as the USA, accounting for more than 54% of all vision loss in the white population [1]. Juvenile macular degeneration (JMD), a term that includes conditions such as Stargardt disease (STGD), fundus flavimaculatus, etc., is similar in pathophysiology to the dry type of AMD, in that a gradual vision loss results from pigment epithelial changes and photo-receptor degeneration and/or loss. Most patients with central vision loss (CVL) develop a non-central retinal locus for fixation, referred to as the 'Preferred Retinal Locus' (PRL) [2, 3]. Although the PRL is outside the central area of obvious retinal damage, it can be surrounded by regions of reduced sensitivity, perhaps due to changes associated with macular degeneration [4–6]. Retinal degeneration in patients with AMD is not restricted to the macula but is usually more widespread, and it is now known that even normal-appearing retinal regions can have deficits in visual functions such as dark adaptation, spatial contrast sensitivity and flicker sensitivity [5, 7, 8].

🖄 Springer

The location of the PRL varies a lot among subjects and primarily depends on the scotoma size and shape [9]. Shima et al. [10] reported that the location of the PRL in a group of 15 subjects with AMD did not coincide with the retinal location of highest sensitivity. Rohrschneider et al. [11] documented that a patch of viable retina exists between the PRL and the central area of degeneration in patients with JMD. In a study by Verdina et al. [12], the PRL in majority of the subjects with STGD was located at a significant distance from the observable edge of the macular atrophy. In contrast, the PRL in patients with AMD is located invariably near the edge of the central scotoma, and shifts more peripherally as the degeneration engulfs greater regions of central retina [13]. In their study of 825 patients with low vision, Fletcher et al. found that roughly 1 in 6 patients have their PRL surrounded by dense scotomas, constraining the usefulness of the PRL for many visual tasks [9, 14].

Micro-perimeters have been used increasingly in the recent past to assess a variety of retinal conditions, including macular degeneration. Because much of the inherent fixation insstability of eyes with CVL can be compensated by the instrument, the results are expected to be more reliable and accurate than those of conventional perimetry [15]. Several groups investigated sensitivity in eyes with macular degeneration over retinal regions with pigmentary changes, drusen [16], flecks [12] and abnormal autofluorescence, but the crucial region around the PRL has not received sufficient attention [5, 17–20]. In this study, we investigate whether regions of reduced sensitivity, which we designate as micro-scotomas (MSs), occur at the fixation PRL in subjects with bilateral CVL. Our protocol differs from the rare-bit vision test employed by Winther & Frisen [21], which presents briefly flashed (150 ms) bright micro-dots (dia. ~0.5′) at random locations and records the percentage of dots seen but not their retinal locations. Identification and mapping of MSs near the PRL of subjects with bilateral CVL is expected to benefit visual rehabilitation, as patients can be trained to use an area of non-central retina [10] with few or no MSs as the PRL for essential visual tasks such as reading and facial recognition.

Methods

Twenty-nine subjects (age: 17–89 years, mean ± SD: 57 ± 21 years, 16 females) with bilateral central vision loss due to conditions such as AMD, STGD, Cone/Cone-rod dystrophy, Macular holes etc. and with best corrected visual acuity in the better eye better than 20/400, were recruited from the Center for Sight Enhancement at the University Eye Institute, University of Houston. Subjects with nystagmus and/or head tremors, or other ocular co-morbidities such as glaucoma or diabetic retinopathy, were excluded. The study protocol was reviewed by the Committee for the Protection of Human Subjects at the University of Houston and all subjects provided written informed consent (or, for subjects who were minors, assent along with parental consent) before participating. The research followed the tenets of the Declaration of Helsinki.

All the outcome measures reported in this study are for the eye with better best-corrected distance visual acuity or for the subject's preferred eye (determined as the eye that the subject did not close when asked to close one eye) if acuity in the two eyes was equal. During testing, the non-tested eye was occluded with an eye patch. A Nidek MP-1 microperimeter (Software Version: 1.7, Nidek Inc., Padova, Italy) was used both to assess fixation and for visual-field testing. Testing required two study visits and was done after pupillary dilation using 1% Tropicamide and/or 2.5% Phenylephrine. The two study visits were at least one week (range: 1–28 weeks) apart.

Visual testing – Visit 1

a) Fixation

The fixation PRL for a 3-letter word approximately sized at each subject's critical print size (based on the outcome of reading assessment done using handheld MN Read Acuity Charts [22]) was assessed using a Nidek MP-1 microperimeter. We do not report the reading outcome here but, briefly, the critical print size was estimated as the smallest print size that the subject could read with maximum speed [23]. Subjects were instructed to use their preferred eye and viewing location to fixate on the central letter of a 3-letter word (See Fig. 1) while ensuring that the whole word remained visible. The word was in dark Courier font, presented on the uniform white background of the MP-1's LCD display (1.27 cd/m^2).

The size of the displayed letters was limited by the pixel resolution of the MP-1's LCD screen (6.5″, 640 × 480 pixels [15]). For instance, a 20/200 (MAR = 10′, letter height 50′) should be ~8.74 pixels high (using ~10.48 pixel/deg. conversion factor). However, in the MP-1 display, it was rounded to be 9 pixels and the actual logMAR acuity was 20/206 (MAR = 10.3′, letter height 51.5′). The actual sizes of the words displayed are listed in the Supplementary Table. At the start of fixation testing, a reference fundus image was captured by the built-in IR-sensitive camera (768 × 576 pixels, 1° ≈ 15.19 pixels) of the MP-1. The examiner then selected a feature-rich region of interest (ROI, 128 × 128 pixels), such as a blood vessel crossing or part of the disc or atrophic margin on the frozen reference image. The ROI was tracked at a sampling rate of 25 Hz (40 ms) during fixation testing. Fixation was usually recorded for a duration of approximately 30 s (Range: 12–55 Seconds). Three assessments of fixation
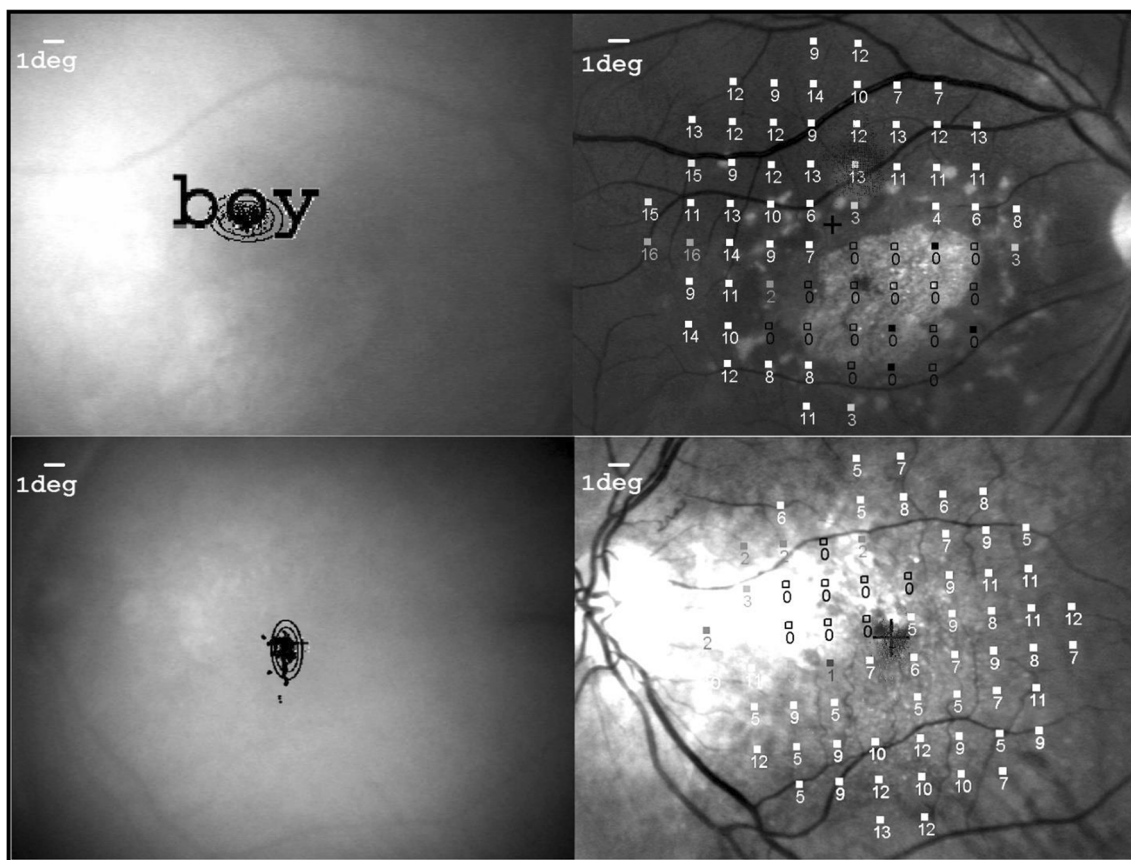
Fig. 1 Fixation and 10–2 Testing. Fixation testing (images on the left) to determine the fixation PRL and 10–2 perimetric testing (images on the right) for subject S3 with STGD (top) and for subject S23 with AMD (bottom). Note that in the left image, the word is flipped vertically (in the retinal view, the word would be inverted) to illustrate the field view. Scale bars are provided in the top left corner of each panel. Letter height was approximately equal to the critical print size, which was 1.3 logMAR (20/400) and 0.8 logMAR (20/125) in S3 and S23 respectively

were obtained successively and the fixation files were exported to compute the bivariate contour ellipse area (BCEA). The latter was calculated, after filtering outliers (±3 SD, to eliminate spurious data points from periods just before and after blinks), using the formula [24]:

$$BCEA = \pi X^2 \sigma_x \sigma_y \sqrt{(1-\rho^2)}$$

BCEA (1SD) was computed offline using a custom MATLAB (R2007a/R2014a - MathWorks, Natick, MA) program. Each subject's median BCEA from the three successive fixation tests and the retinal region corresponding to this contour ellipse were used to perform sensitivity screening on the second study visit.

Marking the location of the PRL During fixation testing, a transparent plastic sheet was placed over the output display screen of the MP-1 to a) trace the retinal features such as blood vessels and the margins of the optic disc and/or atrophic macula and b) mark the approximate

boundaries and center of the fixation PRL. The latter was usually done during the last leg of fixation testing. This transparency was used during the second study visit to help center the test grid at the location of the PRL. The repeatability of positioning the test array using the transparency was assessed by placing a 9 × 9 test grid, 6 times at an IR image location designated as the fixation PRL. Based on the transparencies with the PRL marking of 4 subjects with CVL (S18, S19, S22 and S28), the grids were centered on a standard IR image that was captured with the lens cap on and without positioning any subject in front of eyepiece. The average of the SDs of the X and Y locations of the center of the grid was: ~ 1.1 IR-image pixels (range: 0.52–1.64), corresponding to ±4.31 arc min.

Eccentricity of the PRL The distance of the center of the PRL with the median BCEA from the center of the optic disc was measured using the overlay grid option of the MP-1. The MP-1 overlays a circular grid centered on the PRL center, and the two authors marked the mutually agreed location of the optic disc center on the MP-1's computer

display. The vertical and horizontal distances from the marked disc center to the center of the PRL were then measured with a ruler. Using reported normative values of the foveal center from the center of the optic disc (15.5° temporal and 1.5° inferior from the optic disc center, (according to Rohrschneider [25]) along with the Pythagorean theorem, the radial eccentricity of the PRL from presumed foveal location was calculated in degrees.

b) Assessment of the Central Visual Field

After fixation testing, central retinal sensitivity in the better (test) eye was assessed using a standard Humphrey 10–2 grid (68 points, 2° apart, 4–2–1 thresholding). Goldmann size II spots (squares of nominal side 13 arc min or 2 × 2 LCD pixels) with a luminance ranging from 0 to 20 dB (127 to 2.54 cd/m^2) were presented on a white background of 1.27 cd/m^2, while subjects maintained fixation on a 1–3° red cross target. Testing began after the subject had adapted for at least 15 min to the dimly lit examination room, as in previous studies [26, 27]. A retinal ROI rich in details with a ROI index of at least 2.5 (range: 2.5–8.0) was chosen from an IR image that was frozen during fixation with the previously determined PRL. The MP-1 automatically centers the 10–2 test grid based on the subject's fixation locus during the initial few seconds (2–5 s) of field testing. Consequently, the center of the test grid may not coincide exactly with the fixation PRL that was documented during fixation testing (See Fig. 1).

Visual testing – Visit 2

c) Supra-threshold Sensitivity Screening (STSS)

Fixation testing was repeated at the start of visit 2, to compare with the location of the fixation PRL that was determined on visit 1. The landmarks recorded on the plastic transparency during visit 1 were used as a guide to assess whether the fixation PRL changed during the follow-up period. No noticeable change occurred in any of the subjects in our sample. Custom MATLAB code was used to design the target grid used to sample sensitivity at the fixation PRL (number of locations range: 23–94). The sampling density (nominally 0.2 or 0.3 deg. center-to-center) and size of the bivariate contour ellipse (1 or 2 SD) sampled were chosen to minimize the total test duration (usually ~15 min) and, hence, avoid fatigue. Thus, the STSS grid for each subject was unique. The grid pattern was designed using the 'pattern editor' option of the MP-1 and the luminance of the test spots was set to 0 dB. The grid was manually positioned to overlay the fixation PRL, using the landmarks from visit 1 as a guide.

A custom grid of Goldmann size II targets (maximum L$_{Spot}$ = 127 cd/m^2, L$_{BG}$ = 1.27 cd/m^2) with a center-to-

center spacing of either nominally 12 or 18 arc min (0.2 or 0.3 deg) was used for the baseline STSS (See Fig. 2). Immediately following the baseline test on the same day, a follow-up test using the same target grid was performed. The MP-1 uses examiner-selected ROIs to automatically register the IR image pairs from the initial and follow-up testing. Following this IR-to-IR image registration, the MP-1 automatically placed the STSS grid at the same retinal location as during the initial test. The registration accuracy of the MP-1 for follow-up testing was evaluated and reported previously [28] to be within ~2 pixels in subjects with CVL. Sensitivity testing with the MP-1 includes catch trials for false positives by projecting 0 dB stimuli once every minute onto the center of the optic disc, designated during set up by the operator (range of total number of catch trials = 5–15). The number of false positive responses in our subjects was always <2. Because we used only 0 dB targets to perform STSS, testing for false negative responses was not possible.

We designate the regions within the PRL at which test spots were consistently not detected as micro-scotomas' (MSs) a) as the Goldmann size II spots we employed are half the diameter of the conventional size III (26 arc min) spots and b) because of the high sampling density that was used. For comparison, peripheral retinal locations (eccentricity range: 2–8°) were screened for MSs in a cohort of 8 subjects (age range: 27–71) with normal vision using a high-density grid of 0 dB test spots.

Image registration: IR-MP-1 images The IR test images were registered offline to minimize the small errors inherent in the MP-1's proprietary image registration. A Generalized Dual Boot strap – Iterative Closest Point (GDB-ICP [29]) algorithm registered the retinal locations of the first and second supra-threshold screening grids during baseline and follow-up testing. The accuracy of the algorithm-based registration was confirmed visually by observing minimum flicker when the two fundus images were alternated rapidly. The 2-D affine coefficients returned by the GDB-ICP algorithm were used to transform and re-plot the locations of the test points during follow-up testing onto the baseline IR image (see Figure 2 – zoomed IR images). A rectangular overlap region (based on the Mean ± 2SD of the previously reported IR image registration errors [28]) of ~37 × 22 arc min or 8 × 5 IR image pixels, was drawn around each prospective MS (0 dB test spot not seen) that was identified during baseline testing. A prospective MS detected during follow-up testing was considered to overlap with a baseline scotoma if the follow-up scotoma fell within this rectangular region of overlap. Only overlapping locations
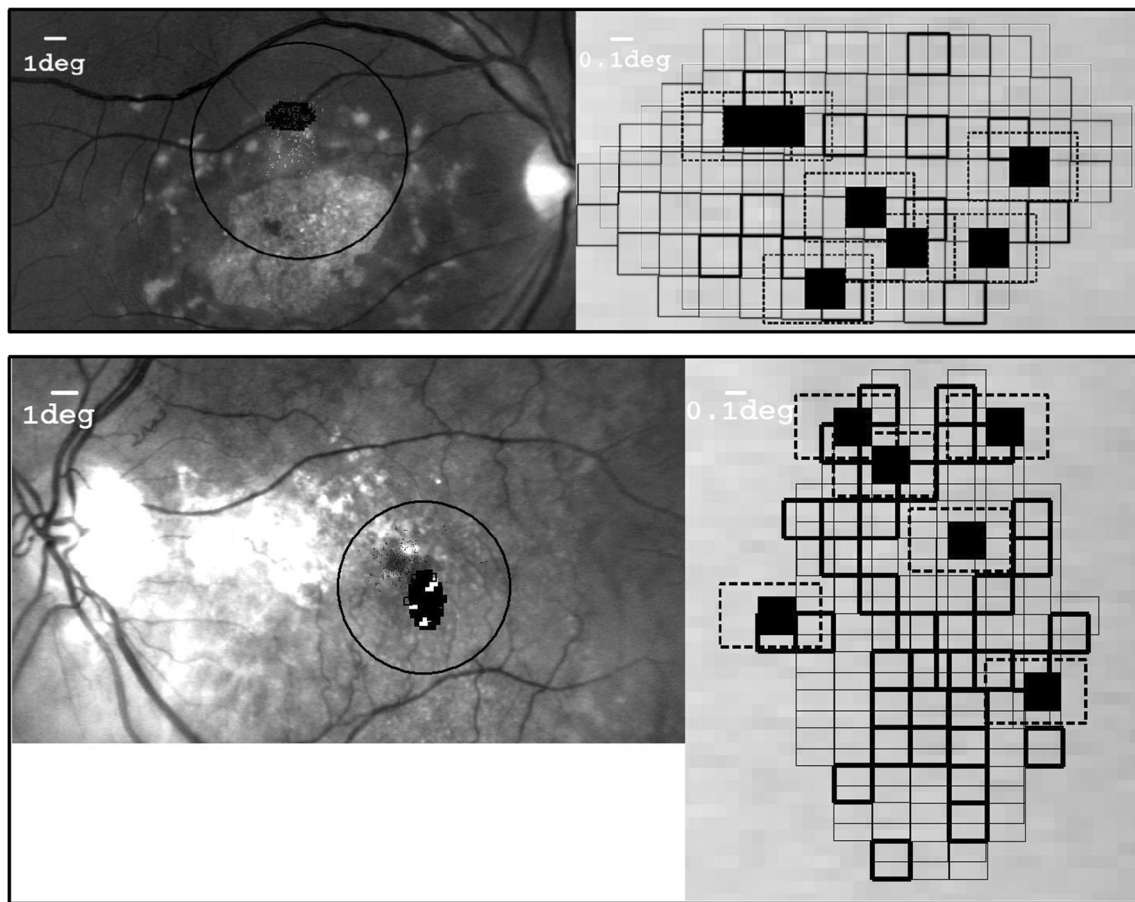
Fig. 2 Supra-threshold screening of the Fixation PRL. Results of supra-threshold screening of the fixation PRL in S3 (STGD, top, $N = 73$) and subject S23 (AMD, bottom, $N = 77$). The customized screening grid was centered on the fixation PRL (left image). The grid (on the right) was re-plotted after offline image registration (to minimize MP-1's image registration errors) using MATLAB. Note the different scale bars in the top left corners. Black filled squares are the locations of test spots not detected on test 1, shown along with 8 × 5 pixel overlap regions - dashed lines) and the thick black squares are the locations of test spots not detected on test 2. MS location counts, defined as the overlapping retinal locations at which a test spot was detected on neither test 1 nor test 2, were 7 and 6 for S3 and S23, whereas definite nonMS location counts, defined as overlapping retinal locations at which the test spot was detected on both test 1 and test 2, were 10 and 2

at which the 0-dB stimulus was not seen on both baseline and follow-up tests are reported here as MSs.

$$
\begin{aligned}
&\text{MS Repeatabilty}\\
&= \frac{\text{Count of test locations with MSs (0 dB target not detected on both tests)}}{\text{Count of test locations with 0 dB target not detected on Test 1}} \times 100\%
\end{aligned}
$$

This expression indicates the percentage of target locations not detected on screening test 1 that also were not detected (within registration accuracy) on screening test 2.

d)　Screening the worse eye

A screening test (6 × 6° grid, 36 locations 1° apart) with 0 dB Goldmann size II spots was performed to confirm the presence of CVL in the non-tested (worse) eye. This screening test, along with the 10–2 testing (Visit 1) described above,

Repeatability of the STSS results was assessed using the following expression:

confirmed that all our subjects had a region of 'absolute' central-retinal scotoma in both the non-preferred and the preferred eyes.

Results

Three fixation assessments were done successively in each subject, and the median bivariate contour ellipse area (68% BCEA) averaged 1.26 ± 1.41 deg^2 (mean ± SD, Range: 0.2–

7.8 deg^2). The BCEAs were *not* significantly different between subjects with AMD vs. STGD (t (20) = 0.80, p = 0.44); AMD vs. Other CVL (t (15) = −0.30, p = 0.77) or STGD vs. Other CVL (t (17) = −0.85, p = 0.41). The average (± SD) radial eccentricity of the fixation PRL from the assumed foveal location was 4.06 ± 2.68° (Range: 0.3–10.15 deg). The radial eccentricities were *not* significantly different between subjects with AMD vs. STGD (t (20) = −1.19, p = 0.25); AMD vs. Other CVL (t (15) = −0.93, p = 0.37) or STGD vs. Other CVL (t (17) = −0.11, p = 0.91). The median BCEA correlated poorly with the radial eccentricity of the fixation PRL (r = + 0.231, p = 0.114, see supplementary Fig. S1). No significant correlation exists between PRL eccentricity and BCEA for AMD (r = +0.524, p = 0.060), STGD (r = −0.131, p = 0.343) or for subjects with other types of CVL (r = + 0.266, p = 0.283).

Across subjects, the average (±SD) of the median (4–6 locations) sensitivity around the fixation PRL from 10–2 testing using the MP-1 was 4.93 ± 4.73 dB. On average, 51 locations (Range: 23–94, see Table 1) around the fixation PRL were screened for MSs. The number of locations that had MSs and the number of nonMS locations varied widely across subjects. Except for a few subjects who had roughly similar numbers of MS and nonMS locations (e.g.: S3, S12), most of our subjects had a highly unequal distribution of MS and nonMS locations. The %MSs had a moderate correlation with the median sensitivity around fixation PRL, determined during earlier 10–2 testing (r = −0.605, p = 0.00051, see supplementary Fig. S2). For the 23 subjects who failed to detect one or more targets on the baseline screening test, the median value of MS repeatability was 93.6% (interquartile range = 73.2% − 100%). The four subjects (1 AMD, 3 STGD) whose values of MS repeatability were in the lowest quartile failed to detect between 3 and 7 targets on screening test 1. Therefore, the calculation of MS repeatability for these 4 subjects is based on relatively small numbers of data points.

Using the same criterion as applied to the subjects with CVL, only one of the 8 subjects with normal vision exhibited a peripheral MS (i.e., 1 of the 492 total locations screened). This lends more credence to the finding of MSs at the PRL of CVL subjects. It is noteworthy that the prevalence of one or more MSs within the PRL was similar for the subjects with AMD (8/10), STGD (10/12) and subjects with other forms of CVL (4/7). Moreover, the average percentage of MSs was similar across the 3 groups with CVL (AMD: 25.4%, Stargardt disease: 20.3%, other CVL: 27.1%). The percentages of MSs were *not* significantly different between AMD vs STGD (t (20) = 0.42, p = 0.68); AMD vs Other CVL (t (15) = −0.13, p = 0.90) or STGD vs Other CVL (t (17) = −0.52, p = 0.61).

Discussion

Fixation stability assessed using BCEA had a poor and insignificant correlation with the eccentricity of the PRL. This is perhaps due to the diverse nature of the subjects, with varying duration of central vision loss in our study, and concurs with other reports of poor correlation in the literature [2, 30]. Interestingly, some studies [24, 31–33] report a significant correlation between the PRL eccentricity and fixation stability, so the relationship is still unclear. The range of BCEA values reported here is similar to other studies of patients with CVL [27, 32, 34, 35]. As speculated previously by others, it is plausible that the duration and stability over time of the CVL has a bearing on the fixational stability [30, 36]. It should be noted that this study was not intended to understand the development of PRL or the course of functional changes at the PRL during disease. The follow-up times we report are only to inform that there was a time gap between 10–2 testing and the STSS. However, it is worth noting that a shift in PRL location during the follow-up period was not observed in any of our subjects.

We report here the novel finding that micro-scotomas occur frequently within the PRL of subjects with CVL. Within our cohort of 29 subjects, 7 exhibited no MSs, whereas the remaining 22 subjects were determined to have MSs at an average of ~25% of the sampled PRL locations (based on our overlap criterion, 1 of the 23 subjects who failed to detect targets on the initial screening test was determined to have no MSs). The distribution of percentages of MSs was very similar across the three subject cohorts with CVL. Because several reports [2, 24, 36] suggested that the PRL in AMD usually is located at the atrophic margin, we anticipated that the AMD cohort would have a higher percentage of MSs than, for example, subjects with Stargardt disease. We did not attempt to demarcate the edges of the atrophic regions in our subjects, as such demarcation can be difficult in non-AMD subjects where the atrophic margins are not very conspicuous. However, using the locations of the absolute central scotomas identified during 10–2 testing as an indicator of the atrophic margin, 9 of the 10 AMD subjects had the PRL at the edge of the atrophic area, whereas only 4 of the 12 subjects with Stargardt disease located their PRL adjacent to the atrophic margin. Imaging modalities such as fundus autofluorescence imaging or optical coherence tomography might have provided better localization of the subjects' atrophic margins. Although AMD and STGD differ in terms of clinical presentation and pathophysiology, eventually photoreceptor damage occurs in both conditions. Regardless of the differences in clinical presentation between these two conditions, we assume that the MSs we identified at our subjects' PRLs are indicative of underlying photoreceptor damage. It would be of interest to screen the

Table 1 Results of Supra-threshold Screening

Subject Code	Diagnosis	Follow-up Time (Weeks)	CPS (MN Read) (logMAR)	BCEA (1SD) (deg²)	Radial Eccentricity (deg)	Median Sensitivity near PRL (dB)	Locations Screened Count	% MS
S1 #	AMD	20.1	0.7	0.20	0.30	0	28	0
S2	AMD	1.4	0.8	2.31	2.98	2.5	67	9.0
S3	STGD	2.4	1.3	1.31	3.73	12.5	73	9.6
S4	STGD	2.0	1	0.57	5.50	8	50	6.0
S5 #	CRD	6.3	1.15	0.85	5.52	10	67	0
S6	STGD	7.9	0.95	0.34	5.07	8	33	3.0
S7 #	PM	4.0	1.2	1.01	10.15	5	37	0
S8	CRD	1.0	0.8	0.25	0.94	0	41	61.0
S9	STGD	1.0	1.1	1.16	7.06	0	37	59.5
S10	AMD	7.6	1.15	0.66	7.85	0	55	10.9
S11	MH	2.6	1.22	0.82	1.76	8.5	29	41.4
S12	STGD	10.0	1.25	1.10	8.93	10	36	13.9
S14 #	STGD	1.0	1.1	0.30	5.60	14.5	23	0
S15	STGD	7.7	1.27	0.46	3.53	13	41	4.9
S16	AMD	3.3	1.4	1.12	0.65	0	33	75.8
S18	STGD	27.7	1.07	1.97	2.06	8.5	57	1.8
S19 #	AMD	2.3	1.1	2.58	8.38	6.5	67	0
S20	PM	4.7	1	7.78	6.71	8	94	36.2
S22	STGD	13.6	1.3	2.07	4.00	0	57	77.2
S23	AMD	7.1	0.8	1.05	3.00	5.5	77	7.8
S25	MMD	1.0	1.2	0.41	5.59	0	37	51.4
S26	STGD	4.1	1.07	0.89	2.00	0	62	62.9
S27	AMD	2.0	1.15	0.45	1.12	2	39	33.3
S28	AMD	5.3	1.175	0.76	1.12	0	62	46.7
S29	AMD	1.0	0.85	0.98	2.50	0	73	67.1
S30 #	STGD	4.7	1.2	0.97	4.03	3	31	0
S31	STGD	2.3	0.875	0.48	2.06	2.5	44	4.6
S32	AMD	0.9	1.175	1.96	4.12	4	62	3.2
S33 #	CD	0.1	0.95	1.86	1.58	11	56	0
	Average	5.3	1.08	1.26	4.06	4.93	50.62	23.69
	SD	6.1	0.18	1.41	2.68	4.73	17.71	27.22

Results from the sensitivity screening test at the fixation PRL. The fourth column reports the critical print size (CPS, letter height in logMAR obtained from MNREAD testing) of the words used for fixation testing. The seventh column reports the median sensitivity of the 4 to 6 test points located around the PRL, from 10-2 testing using nominal Goldmann size II spots and a 4-2-1 thresholding strategy

The subject codes for the seven subjects (2 AMD, 2 with Stargardt disease [STGD], and 3 with other etiologies of central vision loss) who were found to have no MSs are identified by underlining and a hash (#) mark. Interestingly, no MSs were identified during supra-threshold screening for subject S1, whose median sensitivity around PRL during 10-2 testing was 0. This is because the number of missed targets in the first supra-threshold screening test was 0. Thus, although S1 failed to detect 6 targets during supra-threshold screening test 2, the number of overlapping missed targets was 0. (Codes for other etiologies of CVL: CRD = cone rod dystrophy, CD = cone dystrophy, PM = Plaquenil maculopathy, MH = macular hole, MMD = myopic macular degeneration). Also, refer to Supplementary Table for actual acuity values that MP-1 can display

PRL in subjects with recent onset CVL to determine if MSs exist even at the time the PRL is being established.

One explanation for the apparently similar mean percentages of MSs in the three cohorts we tested is that our region-of-overlap criterion for undetected target locations on the initial and follow-up STSS tests was excessively large, and that some of the MSs classified based on overlapping missed test locations were not necessarily overlapping. In other words, we might have over-estimated the percentages of MSs in some subjects. In seven subjects (3 AMD, 3 STGD, 1 with macular hole) all the tested locations within the PRL exhibited MSs. On the other hand, two of the subjects with AMD, two of the subjects with STGD and two subjects with other etiologies of CVL had no identified MS locations within the PRL. Despite the fact that most of the subjects (8 of 12 in our study) with STGD adopt a PRL that is remote from the margin of the atrophic macula, the high prevalence of MSs in these subjects leads us to conclude that retinal function at the PRL is abnormal in the majority of subjects with STGD [6].

Limitations of the study All the assessments performed in this study were monocular and so may not reflect the real-world situation of our subjects, which is almost always binocular. Although both the scanning laser ophthalmoscope (SLO) and commercially available micro-perimeters are monocular instruments, an optical attachment to a SLO was demonstrated to be effective in imaging both eyes simultaneously [37]. The

location of the PRL, which can differ across tasks, [38] has been estimated to be at corresponding retinal locations in the two eyes of subjects with CVL [39]. Weicek, Jackson & Bex, [40] reported a binocular micro-perimetry system employing eye tracking and stereo shutter glasses that reliably mapped the location of simulated scotomas in normally-sighted subjects. With these new technologies, it will be of interest to explore functional changes at the binocular PRL. On a different note, although our measure of MS repeatability indicates good internal consistency, we did not follow our subjects over time. To know if MSs at the fixation PRL are stable and replicable over time, a future study would need to probe the fixation PRL over multiple testing visits. Nevertheless, our study provides one of the first pieces of evidence for local functional changes at the fixation PRL in patients with central vision loss.

Conclusions

The PRL for fixation in subjects with macular degeneration (AMD, Stargardt disease and subjects with other etiologies of central vision loss) frequently includes local regions of sensitivity loss, or MSs. Probing the PRL and the region surrounding the PRL, including the margin of the central atrophic region, has the potential to provide useful information about patients' current visual capabilities and limitations, to improve the monitoring of treatments and interventions, especially in patients with wet AMD, and to assist in the selection and training of an appropriate eccentric viewing locus.

Compliance with ethical standards

Conflict of interest Both authors certify that they have no affiliations with or involvement in any organization or entity with any financial interest (such as honoraria; educational grants; participation in speakers' bureaus; membership, employment, consultancies, stock ownership, or other equity interest; and expert testimony or patent-licensing arrangements), or non-financial interest (such as personal or professional relationships, affiliations, knowledge or beliefs) in the subject matter or materials discussed in this manuscript.

Ethical approval All procedures performed with the human subjects who participated in this study were in accordance with the ethical standards of the institutional research committee at the University of Houston and with the 1964 Helsinki declaration and its later amendments.

Informed consent Informed consent was obtained from all individual participants included in the study.

References

1. Smith W, Assink J, Klein R et al (2001) Risk factors for age-related macular degeneration: pooled findings from three continents. Ophthalmology 108:697–704

2. Timberlake GT, Mainster MA, Peli E et al (1986) Reading with a macular scotoma. I. Retinal location of scotoma and fixation area. Invest Ophthalmol Vis Sci 27:1137–1147

3. Crossland MD, Engel SA, Legge GE (2011) The preferred retinal locus in macular disease: toward a consensus definition. Retina 31: 2109–2114

4. Cideciyan AV, Swider M, Aleman TS et al (2005) ABCA4-associated retinal degenerations spare structure and function of the human parapapillary retina. Invest Ophthalmol Vis Sci 46: 4739–4746

5. Rogala J, Zangerl B, Assaad N et al (2015) In vivo quantification of retinal changes associated with drusen in age-related macular degeneration. Invest Ophthalmol Vis Sci 56:1689–1700

6. Maia-lopes S, Silva ED, Silva MF et al (2008) Evidence of widespread retinal dysfunction in patients with Stargardt disease and morphologically unaffected carrier relatives. Invest Ophthalmol Vis Sci 49:1191–1199

7. Hogg RE, Chakravarthy U (2006) Visual function and dysfunction in early and late age-related maculopathy. Prog Retin Eye Res 25:249–276

8. Curcio CA, Owsley C, Jackson GR (2000) Spare the rods, save the cones in aging and age-related maculopathy. Invest Ophthalmol Vis Sci 41:2015–2018

9. Fletcher DC, Schuchard RA (1997) Preferred retinal loci relationship to macular scotomas in a low-vision population. Ophthalmology 104:632–638

10. Shima N, Markowitz SN, Reyes SV (2010) Concept of a functional retinal locus in age-related macular degeneration. Can J Ophthalmol 45:62–66

11. Rohrschneider K, Bültmann S, Springer C et al (2008) Use of fundus perimetry (microperimetry) to quantify macular sensitivity. Prog Retin Eye Res 27:536–548

12. Verdina T, Tsang SH, Greenstein VC et al (2012) Functional analysis of retinal flecks in Stargardt disease. J Clin Exp Ophthalmol 86: 390–393

13. Fujita K, Yuzawa M (2003) Preferred retinal locus in patients with age-related macular degeneration. Nippon Ganka Gakkai Zasshi 107:602–606

14. Fletcher DC, Schuchard RA, Watson G (1999) Relative locations of macular scotomas near the PRL: effect on low vision reading. J Rehabil Res Dev 36:356–364

15. Midena E, Radin PP, Convento E (2006) Liquid crystal display microperimetry. In: Midena E (ed) Perimetry and the fundus: An intoduction to microperimetry, 1st edn. Slack, Thorafare (New Jersey), pp 15–25

16. Hartmann KI, Bartsch DU, Cheng L et al (2011) Scanning laser ophthalmoscope imaging stabilized microperimetry in dry age-related macular degeneration. Retina 31:1323–1331

17. Iwama D, Tsujikawa A, Ojima Y et al (2010) Relationship between retinal sensitivity and morphologic changes in eyes with confluent soft drusen. Clin Exp Ophthalmol 38:483–488

18. Yehoshua Z, Rosenfeld PJ (2012) Strategies for following dry age-related macular degeneration. Ophthalmic Res 48:6–10

19. Sulzbacher F, Kiss C, Kaider A et al (2012) Correlation of SD-OCT features and retinal sensitivity in neovascular age-related macular degeneration. Invest Ophthalmol Vis Sci 53:6448–6455

20. Midena E, Vujosevic S, Convento E et al (2007) Microperimetry and fundus autofluorescence in patients with early age-related macular degeneration. Br J Ophthalmol 91:1499–1503

21. Winther C, Frisen L (2015) New rarebit vision test captures macular deficits hidden to acuity tests. Acta Ophthalmol 93:481–485

22. Mansfield JS, Legge GE, Luebker A, Cunningham K (1994) MNREAD Acuity Charts. Lighthouse Low Vision Products, Minneapolis, http://www.aureliecalabrese.com/wp-content/uploads/2017/01/mnread.pdf Accessed 7 Sep 2017

23. Mansfield S, Legge GE, Bane MC (1996) Psychophysics of reading XV: Font effects in normal and low vision. Invest Ophthalmol Vis Sci 37:1492–1501

24. Timberlake GT, Sharma MK, Grose SA et al (2005) Retinal location of the preferred retinal locus relative to the fovea in scanning laser ophthalmoscope images. Optom Vis Sci 82:177–185

25. Rohrschneider K (2004) Determination of the location of the fovea on the fundus. Invest Ophthalmol Vis Sci 45:3257–3258

26. Midena E, Vujosevic S, Cavarzeran F et al (2010) Normal values for fundus perimetry with the microperimeter MP1. Ophthalmology 117:1571–1576

27. Longhin E, Convento E, Pilotto E et al (2013) Static and dynamic retinal fixation stability in microperimetry. Can J Ophthalmol 48:375–380

28. Krishnan A, Patel NB, Stevenson SB, Bedell HE (2014) Registration accuracy of NIDEK MP-1 micro-perimeter in "follow-up" testing. Invest Ophthalmol Vis Sci 55:6113

29. Yang G, Stewart CV, Sofka M, Tsai CL (2007) Registration of challenging image pairs: Initialization, estimation, and decision. IEEE Trans Pattern Anal Mach Intell 29:1973–1989

30. White JM, Bedell HE (1990) The oculomotor reference in humans with bilateral macular disease. Invest Ophthalmol Vis Sci 31:1149–1161

31. Nguyen-Tri D, Faubert J, Seiple WH, Overbury O (2016) Fixation stability as a function of preferred retinal locus eccentricity. Invest Ophthalmol Vis Sci 57:5173

32. Bedell HE, Pratt JD, Krishnan A et al (2015) Repeatability of Nidek MP-1 fixation measurements in patients with bilateral central field loss. Invest Ophthalmol Vis Sci 56:2624–2630

33. Reinhard J, Messias A, Dietz K et al (2007) Quantifying fixation in patients with Stargardt disease. Vis Res 47:2076–2085

34. Macedo AF, Crossland MD, Rubin GS (2011) Investigating unstable fixation in patients with macular disease. Invest Ophthalmol Vis Sci 52:1275–1280

35. Seiple W, Rosen RB, Garcia PM (2013) Abnormal fixation in individuals with age-related macular degeneration when viewing an image of a face. Optom Vis Sci 90:45–56

36. Crossland MD, Culham LE, Kabanarou SA, Rubin GS (2005) Preferred retinal locus development in patients with macular disease. Ophthalmology 112:1579–1585

37. Timberlake GT, Ward W (2013) Optical attachment for binocular imaging with the Scanning Laser Ophthalmoscope (SLO). Invest Ophthalmol Vis Sci 54:2182

38. Crossland MD, Crabb DP, Rubin GS (2011) Task-specific fixation behavior in macular disease. Invest Ophthalmol Vis Sci 52:411–416

39. Tarita-Nistor L, Eizenman M, Landon-Brace N et al (2015) Identifying absolute preferred retinal locations during binocular viewing. Optom Vis Sci 92:863–872

40. Wiecek EK, Lou JM, Bex PJ (2015) Binocular microperimetry with simulated asymmetric bilateral scotomas. Invest Ophthalmol Vis Sci 56:549